DE GRUYTER OPEN

Are the phosphorus-rich Na_2O–CaO–B_2O_3–SiO_2–P_2O_5 glasses bioactive and what is an influence of doping with manganese oxide?

P. Bragiel[1,*], P. Ficek[1], W. Prochwicz[2], I. Radkowska[1], N. Veeraiah[3]

[1]Institute of Physics, Jan Dlugosz University, Czestochowa, Poland

[2]Institute of Chemistry, Environmental Protection and Biotechnology, Jan Dlugosz University, Czestochowa, Poland

[3]Physics Department, Acharya Nagarjuna University, Nagarjuna Nagar-522 510, A.P., India

A series of glasses of the composition $20Na_2O$–$15CaO$–$5B_2O_3$–$5SiO_2$–$(55 - x)$ P_2O_5:$xMnO_2$, was prepared and characterized by XRD, DSC, SEM, and Raman techniques. The samples were later immersed in simulated body fluid (SBF) for checking the potential growth of hydroxyapatite layer (HA). Experiments confirmed that addition of manganese oxide leads to structural changes of the glasses. With increasing content of MnO_2, the surface of the samples became more congenial for improving the growth of HA. The formation of HA layer on the surface of the samples was confirmed just after seven days of immersion. The growth rate of HA has gradually increased with the increase of MnO_2 content.

Keywords: *bioactive glass; Simulated Body Fluid; Mn ions as dopant; hydroxyapatite grains shape*

1. Introduction

After almost fifty years from the date of the first publication by Hench, concerning bioactive glassy material, the number of patients benefited from using this type of materials as implants is counted in millions [1, 2]. The most popular and widely used, without any doubts, is the original Hench glass: 45 % SiO_2 – 24.5 % Na_2O – 24.5 % CaO – 6 % P_2O_5, known as 45S5 or Bioglass. Now it is sold under different commercial brands, depending on the size of glass particles and the type of diseases it is dedicated for [3]. Bioactive glasses are present even in popular dental care products, especially those for so-called sensitive teeth [3]. It is expected that an active material will be strongly joined to a bone tissue. To fulfill this requirement, it is necessary for the glass surface to stay coated by the hydroxyapatite (HA) or hydroxycarbonate apatite (HCA) layer after placement in body fluids. Only surface prepared in such way occurs to be a good place for colonization by osteoblasts,

bone tissue cells. Growing of the HCA layer is connected with a degradation of the glass. An explanation of ions exchange between the glass and the body fluid was given by Hench [4], and it included all the necessary steps leading to HCA layer formation. The crucial point seems to be lowering the number of bonding oxygens due to an exchange of O–Si–O units for O–Si–Na ones. This results in lower polymerization of silica tetrahedrons network, lower viscosity of the glass and its higher solubility. The next important step is the formation of silanols (–Si–OH) that cover the glass surface. This explanation is clearly valid for silica active glassy materials.

Maybe this explanation of the chemistry of bioactive glasses, in which silicon atoms play a crucial role, is one of the reasons why the researcher's attention has mostly been concentrated on that kind of glasses. Different silica glass compositions were studied [3], and it was established that SiO_2 content has to be between 40 wt.% and 55 wt.%; above the last value bioactivity is limited [1, 3]. These borders are valid for glasses obtained using melt quenching method; in case of less

---

*E-mail: p.bragiel@ajd.czest.pl

dense, more porous, sol-gel method prepared materials, the bioactivity was observed for the glass containing over 70 wt.% of silica [5].

While the knowledge about bioactive glassy materials built on silica based structures is rather wide, glasses prepared with other glass forming materials have rarely been considered. If we focus on phosphorus glasses, studies by Ahmed et al. [6] and by Rahman et al. [7] may be considered as representative. The active glass studied by them has high P_2O_3 content, $71P_2O_5–19.7CaO–9.3NaO_2$, and phosphorus oxide is the only glass former.

In case of silica glasses which contain a small amount, up to a few wt.%, of P_2O_5, it was observed that there were two independent glass networks, i.e. phosphorus tetrahedrons were not built into silicon network. This is often considered in thermoanalytical studies as a double glass transition effect; it was also explained on the basis of theoretical analysis of the glass networks [8].

The next problem which should be considered as connected with bioactivity is the influence of dopants, especially transition metals. Some of the metals were tested, among them: Zn, Mg, Sr, Cu, and Co [9–13]. The general conclusion from these investigations is that introduction of additional metal improves bio-properties of the glass. For example, *in vitro* experiments with osteoblasts settled on the glass samples, clearly revealed that the presence of Cu ions in the glass raised the speed of osteoblast proliferation and also supported angiogenesis [9]. This way, the Cu-doped glass offers better conditions for rebuilding of a bone tissue.

If we consider all the facts mentioned above, it is obvious that more attention should be paid to P_2O_5 bioactive glasses as well as to transition metal dopants acting as an activating factor. The poor chemical durability of the phosphate glasses, which usually limits their applications, may be an advantage in this case.

The aim of the study reported here was to check if the glass built mainly from phosphorus units, containing only a few percent of silicon dioxide, would exhibit promising properties during *in vitro* test in SBF and what is the influence

of different amounts of MnO_2 added to the glass mixture on the structure and volume of the phosphate layers growing on their surfaces. The composition of the tested glass was: $20Na_2O–15CaO–5B_2O_3–5SiO_2–(55 – x)P_2O_5{:}xMnO_2$.

2. Experimental

The material was prepared by melt quenching method. The composition of the glass was chosen so as to illustrate a reverse of a typical relation between SiO_2 and P_2O_5 content in bioactive glasses. The detailed compositions of the glasses are summarized in Table 1.

Table 1. Composition of the investigated glasses (data given in wt.%).

Glass	CaO	Na₂O	SiO₂	B₂O₃	P₂O₅	MnO₂
PG0	15	20	5	5	55.0	0.0
PG1	15	20	5	5	54.9	0.1
PG2	15	20	5	5	54.8	0.2
PG3	15	20	5	5	54.7	0.3
PG4	15	20	5	5	54.6	0.4
PG5	15	20	5	5	54.5	0.5
PG8	15	20	5	5	54.2	0.8
PG10	15	20	5	5	54.0	1.0

The stoichiometric amounts of proper oxides were grinded in a mortar and melted in an electrical furnace. The melt was kept for thirty minutes at 1400 °C and quenched at room temperature. After quenching it was transferred to another furnace where it was held at 350 °C for twelve hours. The samples were cut off in form of 2 mm thick plates and polished to optical quality All the glasses, despite the one containing MnO_2, are transparent: one of glass pieces is shown in Fig. 1 as an example.

The glassy state of the obtained material was verified with XRD pattern. Diffractograms were recorded with Cu-Kα radiation on URD-6 X-ray diffractometer. Glass transition temperatures were obtained from differential scanning calorimetry (DSC) data. They were registered on Netzsch STA 409C analyzer. The heating rate was 10 K/min.
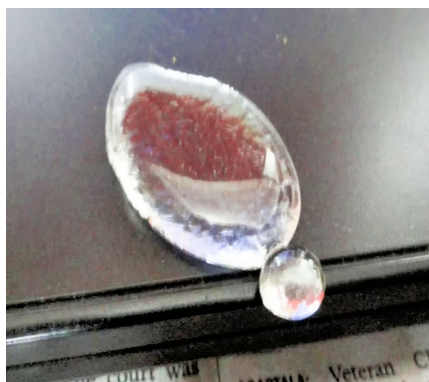
Fig. 1. An example of a piece of glass obtained from the melt quenching.

The samples were kept in corundum crucibles, in an argon atmosphere. Raman spectra were recorded at ambient temperature on Bruker Vertex 55 spectrometer, the resolution was 4 cm^{-1} and the laser line of 532 nm was used for excitation. A structure of the samples surfaces and near surface area was investigated with Vega Tescan scanning electron microscope. The samples were divided into two group. The first group included as obtained samples, the second one contained samples after immersion in a simulated body fluid (SBF). The SBF, artificial human plasma, was prepared according to the procedure described by Oyane and his co-workers [14]. The chemicals used for this purpose, supplied by Sigma-Aldrich and by Avantor Performance Materials (formerly POCH), were of a grade "pure for analysis." The SBF was buffered with tris(hydroxymethyl) aminomethane to keep pH at the level 7.4 ± 0.2.

The samples were immersed during seven, fourteen and twenty one days. The SBF temperature was maintained at 37 °C in a water bath and the SBF was changed to the fresh one every 48 h. After the immersion period, the samples were taken out from the solution and dried.

3. Results and discussion

3.1. Density of the glasses

The density of the glasses was measured using Archimedes method, o-xylene was used as a buoyant. The obtained results are given in Table 2.

Table 2. Densities of the studied glasses.

Glass	Density [g/cm^3]
PG0	2.5910
PG1	2.5605
PG3	2.6218
PG4	2.5977
PG8	2.5542
PG10	2.7154

The density values in Table 2 are in the range typical of bioactive glasses. Hence, we may expect these glasses are prone to be easily degradable. The highest density is for PG10, and the lowest is for PG8. It should be mentioned that the observed changes in densities did not only result from the substitution of P_2O_5 with MnO_2, but also due to the change of the average molar volume of the material.

3.2. XRD

XRD diffractograms verify the amorphous state of the samples. There are no peaks in the patterns. Some examples are shown in Fig. 2.
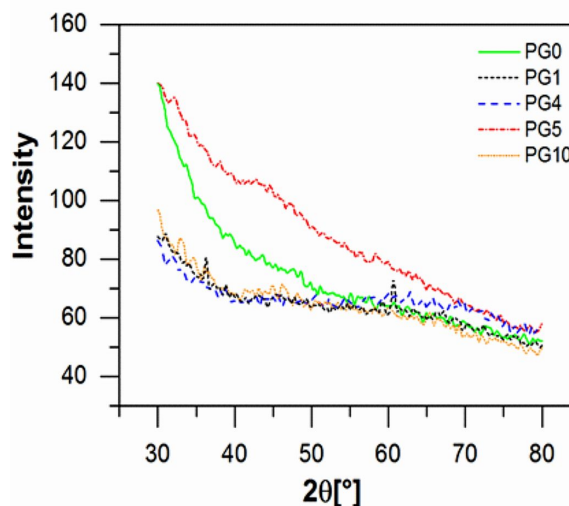

Fig. 2. XRD patterns recorded for the selected glasses.

3.3. Raman spectra

In Fig. 3, Raman spectra of two of samples, the PG0 (the bare glass) and PG10 (the sample with 1 % of MnO_2) are presented.
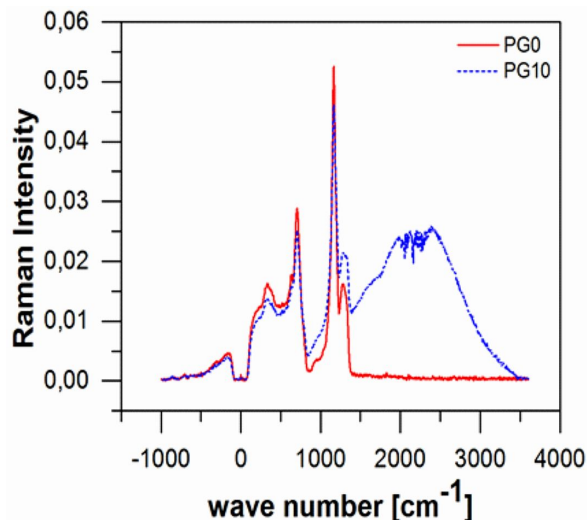
Fig. 3. Raman spectra of PG0 and PG10 samples.

In the studied material, the main glass forming material is P_2O_5, the glass network is composed of PO_4 tetrahedrons. B_2O_3 participates in the glass network with BO_4 and BO_3 units; there may also be B–O–P structure units in the network. It is known that the degree of the network polymerization is growing when P–O–P and B–O–B units are replaced with P–O–B ones [15]. According to the literature reports [16, 17], the peak observed at 1279 cm^{-1} is due to the asymmetric stretching vibrations in PO^{2-} units, coupled with BO_3 vibrations. Another band, observed at 1165 cm^{-1}, is due to symmetric vibrations of PO_4^{3-} units. The band observed at 703 cm^{-1} is attributed to symmetric stretching of P–O–P bonds in PO_4^{3-} tetrahedral chains. The origin of the lower energy bands observed at 596 cm^{-1} and 333 cm^{-1} is not clear; they are probably connected with vibrations inside the Ca–P–O and Na–P–O units.

Addition of manganese oxide leads to a new part of the spectrum: broad and complex peak between 1700 cm^{-1} and 3000 cm^{-1}. It should not be considered as connected with the movements inside the MnO_2 units. The studies on manganese compounds have shown that this type of vibrations is observed in the region of 400 cm^{-1} to 600 cm^{-1} [18]. Thus, this peak has to be due to manganese interactions with the other parts of the glass network. The most straightforward picture is

made by the units O–P–Mn and O–B–Mn. If this is really the case, it means that Mn addition reduces the number of binding oxygens, lowering the degree of the glass network polymerization and increasing the ability of glass degradation.

3.4. Glass transitions

The glass transition temperatures are practically not influenced by MnO_2 addition. For all the investigated glasses the values of T_g are nearly 620 K (Table 3). T_g values given in Table 3 are temperature onsets of endothermic S-type deviation observed in the DSC plots. The relatively low value of T_g suggests that the studied glass is convenient for use in preparation of bioactive scaffolds. There are no crystallization peaks in the DSC patterns. The next deviation from the baseline is observed at about 700 K; it is an endothermic effect.

Table 3. Glass transition temperatures and specific heat change within the transition region.

Glass	T_g [K]	ΔC_p [J/g]
PG0	612.5	0.19
PG1	621.5	0.11
PG2	621.5	0.31
PG3	619.5	0.09
PG4	621.1	0.08
PG8	619.2	0.65
PG10	620.9	0.65

It is possible that in the same temperature range two processes take place: crystallization, which is connected with exothermic effect and stronger endothermic process. We observe only the resultant signal. However, even in this case, there is about 75 K interval between T_g and the next thermal event, pretty enough for sintering process.

3.5. Surface and near surface area

To check the manganese influence on the properties of the glass, we verified the surface structure of the glasses containing different amounts of the dopant. Analysis of the SEM pictures indicates that the surface structures were gradually changing with increasing content of MnO_2. This is illustrated in Fig. 4 and Fig. 5. These figures

present SEM pictures of PG0 and PG10 glasses. The bare glass, PG0, looks very compact, with the uniform surface; the addition of manganese changed this picture. The cauliflower-like structures are observed on the surface of the sample. Up to 0.3 wt.% of manganese oxide, the size of this "flowers" increased with the growing dopant content. The further increase has not changed the size. Dimensions of the structures observed in PG3 and PG10 are the same. What is different is the number of pores on their surfaces. For the glasses PG0, PG1, PG2 there are no pores seen on the surfaces. On the surface of PG3 glass, one pore per 100 μ^2 on average was found while on the surface of PG10 there were about 50 pores per 100 μ^2. The pores are the ends of tubes leading inside the bulk of the glass which is easy to be seen on a photograph taken with higher magnification (Fig. 5). When such tubes are present, penetration of fluids – SBF or blood plasma – in the *in vitro* and *in vivo* experiments is easier. The area of ions exchange is growing, causing that the scale of this process increases. This should result in higher rate of HA layer building and better biodegradability of the glass. From the point of view of expected properties of the biomaterials, this means that addition of MnO_2 makes them better.
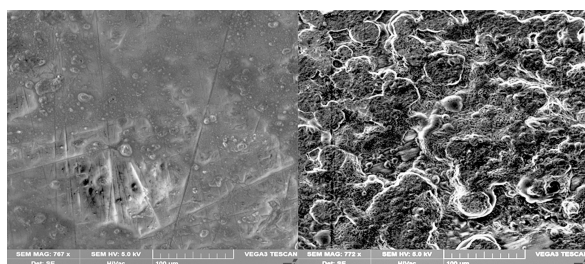

Fig. 5. SEM picture of the PG10. Magnification: ×6000.

Fig. 4. SEM pictures of the PG0 – left and PG10 – right. Magnification 770 times.

3.6. Structure of hydroxyapatite layer

The ability of investigated glasses to create HA layer were verified during the immersion experiment. The samples were immersed in c-SBF for a period of 7 days to 21 days. Even after only seven days in SBF, noticeable changes on the surface were obse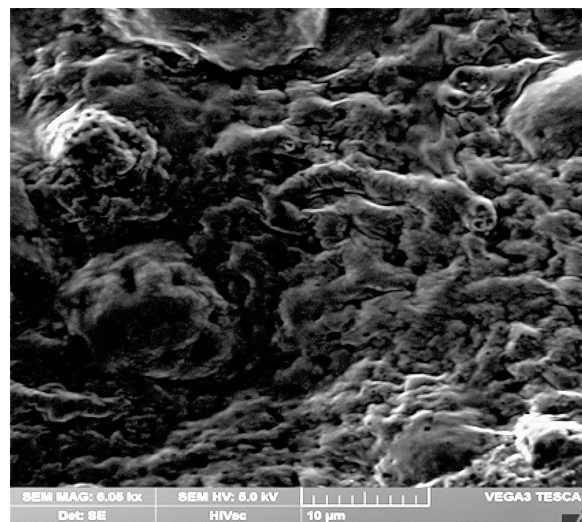rved. The grains of HA were found on the glasses surfaces. On the surface of the glass GP0 there are visible small grains (Fig. 6); with the increase of manganese content the size of grains gradually increases. After a prolonged time of immersion in SBF, the surfaces are covered with HA layers. It looks like as the apatite layers have been growing layer by layer and a lack of ideal fitting led to the breaks in the HA film. On the surface of the glasses with low manganese content, the HA layer is built in the form of plates, whereas on the surface of the glasses containing a higher content of MnO_2 the bubble-shaped structures appear (Fig. 7). Further, the bubbles look like growing from the underlying layer of apatite. Despite the shape of the surface structures – single layers or layers with additional bubble structures on them – it was proved that immersion in SBF leads to glass surfaces covered with new material.

The above-described pictures only prove that something was grown on the surface, but it is not the evidence for HA. XRD patterns revealed that the chemical composition of the formed layers is just HA. Fig. 8 presents the XRD pattern of the PG4 sample after 21-day immersion in SBF. Three diffraction peaks at 32°, 46° and 76° are seen which are due to the (2 2 0) (4 0 0) and (2 0 5) reflections, characteristic of HA layer [19, 20].
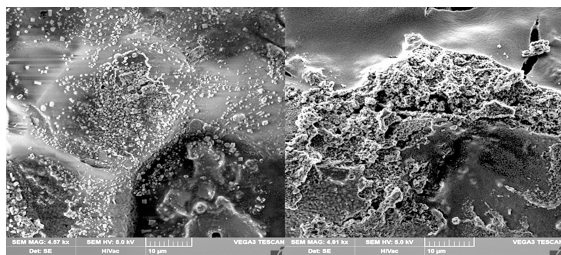
Fig. 6. SEM pictures of glasses surfaces after seven days in SBF. PG0 is on the left, PG10 is on the right.
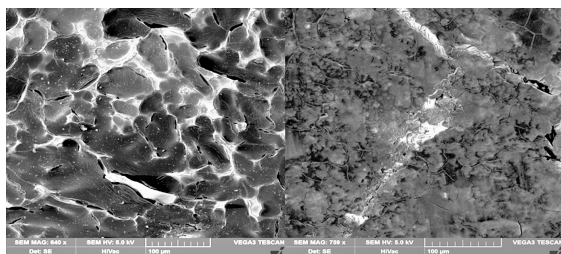

Fig. 7. SEM pictures of glasses surfaces after 21 days in SBF. PG1 is on the left, PG4 is on the right.

4. Conclusions

Glasses of the composition $20Na_2O–15CaO–5B_2O_3–5SiO_2–(55 – x)P_2O_5{:}xMnO_2$, appeared to be a promising bioactive material. When they are immersed in c-SBF, their surfaces are covering

Fig. 8. XRD spectrum of the PG4 glass after 21 days in SBF.

with a hydroxyapatite layer. The structure of the layer and the way of its growth is correlated with the content of MnO_2 in the glass. The higher the amount of manganese in the glass the higher the rate of HA growth.

Most likely it is correlated with increasing porosity and the number of the tubs leading from the surface to inside of the bulk. Also, the structure of the growing HA layers strongly depends on the MnO_2 amount. When there is more than 0.3 wt.% of this compound in the glass, bubbles of HA dominate on the surface. They spread and finally create the layer. For lower dopant content, HA plates occur in the first step. They extend and finally cover all the surface leaving cracks on the borders between them. It may be assumed that the bubble structure, offering bigger HA surface, will be better for colonization with osteoblasts. However, another factors should also be considered. Degradation of the glass is more rapid when it contains a higher amount of the dopant. This leads to a slight acidity of the solution and may stop the proliferation of the cells.

Summarising, the studied glasses behave very well in the SBF bath. The first traces of HA have been observed after several hours, after fourteen days the samples surfaces have covered with multilayer HA coating. This is a promising result which justifies further experiments with osteoblast cells.

References

[1] HENCH L.L., *J. Mater. Sci.-Mater. M.*, 17 (2006), 967.

[2] HENCH L.L., SPLINTER R.J., ALLEN W.C., GREENLEE T.K., *J. Biomed. Mater. Res. A*, 5 (1971), 117.

[3] JONES J.R., *Acta Biomater.*, 9 (2013), 4457.

[4] HENCH L.L., POLAK J.M., *Science*, 295 (2002), 1014.

[5] LEI B., CHEN X.F., WANG Y.J., ZHAO N.R., DU C., FANG L.M., *J. Biomed. Mater. Res. A*, 94A (2010), 1091.

[6] AHMED I., LEWIS M., OLSEN I., KNOWLES J.C., *Biomaterials*, 25 (2004), 491.

[7] RAHMAN M.N., DAY D.E., BAL B.S., FU Q., JUNG S.B., BONEWALD L.F., TOMSIA A.P., *Acta Biomater.*, 7 (2011), 2355.

[8] EDEN M., *J. Non-Cryst. Solids*, 357 (2011),1595.

[9] WU C., ZHOU Y., XU M., HAN P., CHEN L., CHANG J., XIAO Y., *Biomaterials*, 34 (2013), 422 .

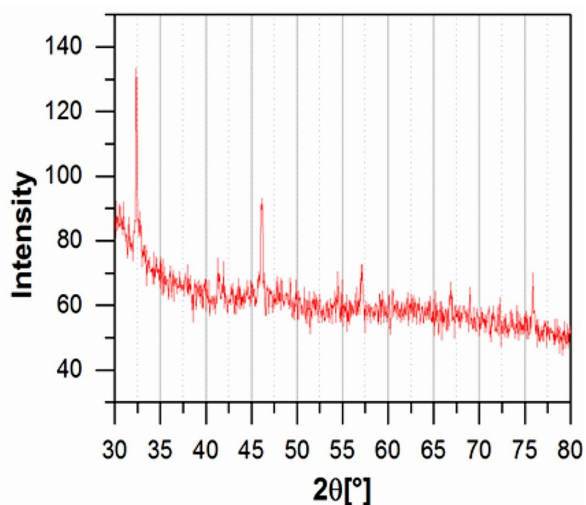[10] WU C., ZHOU Y., FAN W., HAN P., CHANG J., YUEN J., ZHANG M., XIAO Y., *Biomaterials*, 33 (2012), 2076.

[11] Zreiqat H., Ramaswamy Y., Chengtie W.U., Paschalidis A., Lu Z.F., James B., Birke O., Mc-Donald M., Little D., Dunstan C.R., *Biomaterials,* 31 (2010), 3175.

[12] Wu C., Zhou Y., Lin C., Chang J., Xiao Y., *Acta Biomater.,* 8 (2012) 3805.

[13] Gentleman E., Fredholm Y.C., Jell G., Lotfibakhshaiesh N., O'Donnell M.D., Hill R.G., Stevens M. M., *Biomaterials,* 31 (2010) 3949.

[14] Oyane A., Kim H-M., Furuya T., Kokubo T., Miyazaki T., Nakamura T., *J. Biomed. Mater. Res. A*, 65 (2003), 188.

[15] Kalpana T., Brik M.G., Sudarsan V., Naresh P., Ravi Kumar V., Kityk I.V., Veeraiah N., *J. Non-Cryst. Solids*, 419 (2015), 75.

[16] Srinivasa Rao P., Ramesh Babu P., Vijay R. , Narendrudu T., Veeraiah N., Krishna Rao D., *Mater. Res. Bull.,* 57 (2015), 58.

[17] Chahine A., Et-Tabioru M., Elbenaissi M., Haddad M., Pascal J.L., *Mater. Chem. Phys.*, 84 (2004), 341.

[18] Julien C., Massot M., Baddour-Hadjean R., Franger S., Bach S., Pereira-Ramos J.P., *Solid State Ionics*, 159 (2003), 345.

[19] Jagan Mohini G., Sahaya Baskaran G., Ravi Kumar V., Piasecki M., Veeraiah N., *Mater. Sci. Eng. C Mater. Biol. Appl.,* 57 (2015), 240.

[20] Maquet V., Boccaccini A.R., Pravata L., Notingher I., Jerome R., *Biomaterials*, 25 (2004), 4185.